The Plant Cell, Vol. 18, 2822–2835, October 2006, www.plantcell.org © 2006 American Society of Plant Biologists

Multiple Upstream Signals Converge on the Adaptor Protein Mst50 in *Magnaporthe grisea* [W]

Gyungsoon Park,[a,1] Chaoyang Xue,[a,1] Xinhua Zhao,[a,1] Yangseon Kim,[a] Marc Orbach,[b] and Jin-Rong Xu[a,2]

[a] Department of Botany and Plant Pathology, Purdue University, West Lafayette, Indiana 47907
[b] Department of Plant Sciences, University of Arizona, Tucson, Arizona 85721

Rice blast fungus (*Magnaporthe grisea*) forms a highly specialized infection structure for plant penetration, the appressorium, the formation and growth of which are regulated by the Mst11-Mst7-Pmk1 mitogen-activated protein kinase cascade. We characterized the *MST50* gene that directly interacts with both *MST11* and *MST7*. Similar to the *mst11* mutant, the *mst50* mutant was defective in appressorium formation, sensitive to osmotic stresses, and nonpathogenic. Expressing a dominant active *MST7* allele in *mst50* complemented its defects in appressorium but not lesion formation. The sterile α-motif (SAM) domain of Mst50 was essential for its interaction with Mst11 and for appressorium formation. Although the SAM and Ras-association domain (RAD) of Mst50 were dispensable for its interaction with Mst7, deletion of RAD reduced appressorium formation and virulence on rice (*Oryza sativa*) seedlings. The interaction between Mst50 and Mst7 or Mst11 was detected by coimmunoprecipitation assays in developing appressoria. Mst50 also interacts with Ras1, Ras2, Cdc42, and Mgb1 in yeast two-hybrid assays. Expressing a dominant active *RAS2* allele in the wild-type strain but not in *mst50* stimulated abnormal appressorium formation. These results indicate that *MST50* functions as an adaptor protein interacting with multiple upstream components and plays critical roles in activating the Pmk1 cascade for appressorium formation and plant infection in *M. grisea*.

INTRODUCTION

The ascomycete *Magnaporthe grisea* is pathogenic to important crops, such as rice (*Oryza sativa*), barley (*Hordeum vulgare*), and wheat (*Triticum aestivum*). Rice blast, caused by this heterothallic haploid fungus, is one of the most severe fungal diseases of rice throughout the world (Valent and Chumley, 1991; Talbot, 2003). *M. grisea* infects rice plants in a manner typical of many foliar pathogens. Germ tubes produced from conidia differentiate into specialized infection structures called appressoria. Conidial and germ tube cells usually collapse after 24 h when appressoria mature (Veneault-Fourrey et al., 2006). The fungus generates enormous turgor pressure in melanized appressoria to physically penetrate the plant surface (Howard et al., 1991; de Jong et al., 1997). In nature, *M. grisea* attacks all aboveground parts of rice plants and causes severe yield losses. In laboratory conditions, root infection of wheat and rice seedlings by *M. grisea* has been observed (Dufresne and Osbourn, 2001; Sesma and Osbourn, 2004).

In the past decade, *M. grisea* has been developed as a model system to study fungal–plant interactions (Dean et al., 2005; Veneault-Fourrey and Talbot, 2005; Xu et al., 2006). Several signal transduction pathways regulating infection-related morphogenesis have been identified in *M. grisea* (Dean, 1997; Xu, 2000; Tucker and Talbot, 2001). Similar to other fungal pathogens (Kronstad et al., 1998; D'Souza and Heitman, 2001; Lee et al., 2003), both the cAMP signaling pathway and mitogen-activated protein (MAP) kinase gene *PMK1* (homologue of *FUS3* and *KSS1* in *Saccharomyces cerevisiae*) play important roles in appressorium development and infectious growth in *M. grisea*. Appressorium formation in *M. grisea* can be induced in germlings attached to hydrophobic surfaces or hydrophilic surfaces in the presence of exogenous cAMP (Lee and Dean, 1993). Several key components of the cAMP signaling pathway are known to be involved in surface recognition (Mitchell and Dean, 1995; Choi and Dean, 1997; Adachi and Hamer, 1998). The Pmk1 MAP kinase is essential for appressorium formation and plant infection (Xu and Hamer, 1996). The *pmk1* deletion mutant fails to form appressoria and grow invasively in rice plants, but it still responds to exogenous cAMP for germ tube tip deformation and formation of apical swollen bodies on the germ tube. Although cAMP signaling and appressorial penetration are dispensable for root infection (Sesma and Osbourn, 2004), the *pmk1* mutant is nonpathogenic in root infection assays in *M. grisea* (Dufresne and Osbourn, 2001). In the past few years, studies in several other plant pathogenic fungi, including *Fusarium graminearum*, *Fusarium oxysporum*, *Botrytis cinerea*, *Claviceps purpurea*, and *Stagonospora nodorum* have shown that the *PMK1* pathway may be well conserved in plant pathogens for regulating appressorium formation and other plant infection processes (Xu, 2000; Mey et al., 2002; Jenczmionka et al., 2003; Solomon et al., 2005).

In a previous study, we identified the MAP kinase kinase (MEK) Mst7 and MEK kinase (MEKK) Mst11 that activate Pmk1 in *M. grisea* (Zhao et al., 2005). Similar to the *pmk1* mutant, the *mst11* and *mst7* deletion mutants are defective in appressorium formation and are nonpathogenic, indicating that the Mst11-Mst7-Pmk1

[1] These authors contributed equally to this work.
[2] To whom correspondence should be addressed. E-mail jinrong@purdue.edu; fax 765-496-6918.
The author responsible for distribution of materials integral to the findings presented in this article in accordance with the policy described in the Instructions for Authors (www.plantcell.org) is: Jin-Rong Xu (jinrong@purdue.edu).
[W] Online version contains Web-only data.
www.plantcell.org/cgi/doi/10.1105/tpc.105.038422

MAP kinase cascade is conserved for regulating infection-related morphogenesis. Mst11 has an N-terminal sterile α-motif (SAM), and it directly interacts with another SAM-containing protein (MG05199.4) named *MST50* (for *M. grisea STE50* homolog; Zhao et al., 2005). In addition to the *S. cerevisiae STE50* gene, *MST50* is homologous to *STE4* in *Schizosaccharomyces pombe* and *ubc2* in *Ustilago maydis* (Barr et al., 1996; Mayorga and Gold, 2001). Although it is not essential for yeast pheromone responses and filamentous growth, Ste50 constitutively interacts with Ste11 and is involved in modulation of Ste11 function during mating, invasive/filamentous growth, and the SHO1-dependent response to hyperosmolarity (Jansen et al., 2001; Ramezani-Rad, 2003; Kwan et al., 2006; Truckses et al., 2006). Ste50 may also contribute to cell wall integrity in vegetative cells (Ramezani-Rad, 2003). In *S. pombe* and *U. maydis*, Ste4 and Ubc2 are involved in mating and other developmental processes (Barr et al., 1996; Mayorga and Gold, 2001).

In this study, we functionally characterized the *MST50* gene in *M. grisea* to better understand the activation of the Mst11-Mst7-Pmk1 MAP kinase cascade. The *mst50* mutant was defective in appressorium formation, sensitive to osmotic stresses, and nonpathogenic on rice seedlings. Expressing a dominant active *MST7* allele complemented the defect of the *mst50* mutant in appressorium formation but not plant infection. Mst50 directly interacted with both Mst11 and Mst7, and the interaction of Mst50 with Mst11 via the SAM domain was essential for regulating appressorium formation. Mst50 also interacted with Ras1, Ras2, Cdc42, and Mgb1 in yeast two-hybrid assays. Expressing a dominant active *RAS2*^{G23V} allele in the wild-type 70-15 but not in the *mst50* deletion mutant stimulated the formation of morphologically abnormal appressoria on hydrophilic or hydrophobic surfaces. In the *pmk1*, *mst7*, and *mst11* mutants, *RAS2*^{G23V} also failed to stimulate appressorium formation. These results indicate that *MST50* plays critical roles in activating the Pmk1 cascade for appressorium formation and other developmental processes in *M. grisea*. Since this MAP kinase pathway is well conserved, *MST50* homologs may have similar functions in many other ascomycetous fungal pathogens.

RESULTS

MST50 Is Essential for Appressorium Formation

Similar to *STE50* and its homologs in other fungi, *MST50* has an N-terminal SAM (residues 67 to 130) and a C-terminal Ras-association domain (RAD; residues 370 to 456). Although the homology between *MST50* and *STE50* of *S. cerevisiae* is limited to the SAM and RAD domains, *MST50* is highly homologous over the entire protein to its homologs from other filamentous ascomycetes, such as NCU00045 of *Neurospora crassa* (60% identity) and FG04101 of *F. graminearum* (63% identity). No known functional motif was identified in the middle region between the SAM and RAD domains of *MST50* (residues 131 to 369).

To determine the function of *MST50*, we generated the gene replacement construct pGP64 in which the entire *MST50* open reading frame (ORF) was replaced by the hygromycin phosphotransferase (*hph*) gene. After transforming the wild-type strain 70-15 with pGP64, an *mst50* deletion mutant MF103 (Table 1) was identified and confirmed by DNA gel blot analyses (data not shown). MF103 grew normally on regular oatmeal agar plates but was reduced in conidiation (Table 2). Conidia produced by MF103 failed to form appressoria (Figure 1A). In 70-15 and the ectopic transformant MF2E, >90% of germ tubes differentiated into appressoria at 24 h on hydrophobic surfaces. Under the same conditions, >50% of MF103 germ tubes underwent tip deformation and developed swollen bodies (Figure 1A), indicating that the *mst50* mutant had no defect in surface recognition. We also assayed appressorium formation on onion epidermal cells (Figure 1A) and rice leaf sheath epidermis. The *mst50* mutant failed to form appressoria on plant surfaces, and no infectious hyphae were observed in MF103 (Figure 1A).

The *mst50* Mutant Is Nonpathogenic

Both spray and injection infection assays with rice seedlings were used to assay the virulence of the *mst50* mutant. On rice leaves sprayed with conidia of the *mst50* mutant MF103, no lesions were observed by 7 d after inoculation (DAI). Under the same conditions, leaves sprayed with 70-15 produced numerous lesions (Figure 1B). On leaves wound-inoculated with MF103, only limited necrosis developed around the wound sites. MF103 failed to cause lesions beyond the wound sites. The *mst50* mutant was also defective in root infection (data not shown). Therefore, similar to the *pmk1*, *mst7*, and *mst11* mutants, the *mst50* mutant was nonpathogenic.

For complementation assays, the wild-type *MST50* gene cloned in pGP85 was transformed into MF103. CMF4 and CMF11 were two of the resulting transformants that had a single copy of pGP85 ectopically inserted in the genome. On hydrophobic surfaces, >90% of the CMF11 germlings developed melanized appressoria (Table 2). Typical blast lesions were observed on leaves inoculated with CMF11 (Figure 1B). In addition, we isolated 23 ascospore progeny from a cross between MF103 (*MAT1-1*) and the wild-type strain Guy11 (*MAT1-2*). Fifteen progeny were susceptible to hygromycin and phenotypically similar to the wild-type strain. All eight hygromycin-resistant progeny were defective in appressorium formation and plant infection, indicating that the defects of the *mst50* mutant cosegregated with the hygromycin resistance marker. Thus, *MST50* is essential for appressorium formation and plant infection in *M. grisea*.

SAM but Not RAD of *MST50* Is Essential for Appressorium Formation and Plant Infection

To determine the function of the SAM and RAD domains, the *MST50*$^{\Delta SAM}$ (pGP82) and *MST50*$^{\Delta RAD}$ (pGP83) mutant alleles (Figure 2A) were constructed and transformed into the *mst50* deletion mutant MF103. Among the resulting zeocin-resistant transformants analyzed by DNA gel blot hybridization, transformants SD1 and RD1 contained a single copy of pGP82 and pGP83, respectively. Similar to the *mst50* mutant MF103, transformant SD1 was defective in appressorium formation and nonpathogenic. Germ tubes produced by SD1 formed subapical swollen bodies on hydrophobic surfaces (Figure 2B). However, appressoria were not formed on plastic cover slips or onion epidermis by transformant SD1 and four other MF103 transformants

Table 1. Wild-Type and Mutant Strains of *M. grisea* Used in This Study

Strain	Genotype Description	Reference
70-15	Wild type, *MAT1-1*	Chao and Ellingboe (1991)
Guy11	Wild type, *MAT1-2*	Chao and Ellingboe (1991)
DA128	*mac1* deletion mutant	Adachi and Hamer (1998)
nn78	*pmk1* deletion mutant of Guy11, *MAT1-2*	Xu and Hamer (1996)
yk18	*pmk1* deletion mutant of 70-15, *MAT1-1*	Zhao et al. (2005)
DA128	*mac1* deletion mutant of Guy11, *MAT1-2*	Adachi and Hamer (1998)
yk86	*mst11* deletion mutant of 70-15, *MAT1-1*	Zhao et al. (2005)
MRD	$MST11^{\Delta RAD}$ in yk86	Zhao et al. (2005)
MF103	*mst50* deletion mutant of 70-15, *MAT1-1*	This study
MF2E	Ectopic transformant of the *MST50* knockout construct	This study
CMF4	MF103 transformed with the wild-type *MST50* allele	This study
CMF11	MF103 transformed with the wild-type *MST50* allele	This study
MA7-5	$MST7^{S212D\ T216E}$ in MF103	This study
MA7-10	$MST7^{S212D\ T216E}$ in MF103	This study
MW15	Wild-type *MST7* (pHZ10) in MF103	This study
SD1	$MST50^{\Delta SAM}$ in MF103	This study
RD1	$MST50^{\Delta RAD}$ in MF103	This study
MHZ8	MF103 transformed with *MST50*-EGFP	This study
MHZ13	MF103 transformed with *MST50*-EGFP	This study
MCX66	$RAS2^{G23V}$ in Guy11	This study
MCZ66	$RAS2^{G23V}$ in 70-15	This study
MHZ66	$RAS2^{G23V}$ in MF103	This study
MRN78	$RAS2^{G23V}$ in the *pmk1* mutant nn78	This study
M7-1	*MST50*-6His and *MST7*-GFP in 70-15	This study
M7-2	*MST50*-6His and *MST7*-GFP in 70-15	This study
H11-6	*MST50*-6His and *MST11*-HA in 70-15	This study
H11-8	*MST50*-6His and *MST11*-HA in 70-15	This study
MCX90	$RAS2^{G23V}$-CAAX (pCX90) in 70-15	This study
MCX91	$RAS2^{S28N}$ with the *RAS2* promoter (pCX91) in 70-15	This study
MCX99	$RAS2^{S28N}$ with the RP27 promoter (pCX99) in 70-15	This study
MHZ90	$RAS2^{G23V}$ in yk86	This study

carrying pGP82. Transformant SD1 failed to cause lesions on healthy rice leaves (Figure 2C) or to colonize rice tissues through wounds (data not shown). By contrast, transformant RD1 expressing the $MST50^{\Delta RAD}$ allele formed melanized appressoria (Figure 2B). Appressoria formed by RD1 were able to penetrate onion epidermal cells and develop infectious hyphae (Figure 2B). Typical blast lesions were observed on rice leaves inoculated with RD1 conidia (Figure 2C). These data indicate that the SAM but not the RAD domain is essential for *MST50* to regulate appressorium formation and plant infection in *M. grisea*.

Exogenous cAMP Stimulates Appressorium Formation in the $MST50^{\Delta RAD}$ Transformant

Although transformant RD1 formed melanized appressoria, it was reduced in the efficiency of appressorium formation on

Table 2. Vegetative Growth and Appressorium Formation by *M. grisea* Strains

Strain	Growth Rate on Oatmeal Agar (mm/day)[a]		Conidiation ($\times 10^4$ Conidia/Plate)	Appressorium Formation (%)
	Regular	+1 M Sorbitol		
70-15 (wild type)	2.4 ± 0.2	1.7 ± 0.1	245.0 ± 52.0	95.0 ± 2.3
MF103 (*mst50* mutant)	2.3 ± 0.3	0.8 ± 0.1	1.4 ± 0.2	0
MF2E (ectopic)	2.3 ± 0.2	1.6 ± 0.1	185.7 ± 13.4	83.2 ± 6.2
CMF11 (*MST50*/*mst50*)	2.3 ± 0.3	1.5 ± 0.1	32.5 ± 7.6	89.5 ± 4.7
MA7-5 ($MST7^{DA}$/*mst50*)	2.5 ± 0.2	1.6 ± 0.1	2.0 ± 0.9	28.4 ± 3.5
MW15 ($MST7^{WT}$/*mst50*)	2.9 ± 0.1	0.7 ± 0.1	1.0 ± 0.2	0
SD1 ($MST50^{\Delta SAM}$/*mst50*)	2.6 ± 0.2	0.5 ± 0.2	0.7 ± 0.2	0
RD1 ($MST50^{\Delta RAD}$/*mst50*)	2.6 ± 0.2	0.6 ± 0.2	2.0 ± 0.7	20.0 ± 3.0

[a] Growth rate was measured in race tubes after 35 d. Average growth rates and standard errors (mean ± SE) were calculated from at least three independent measurements.

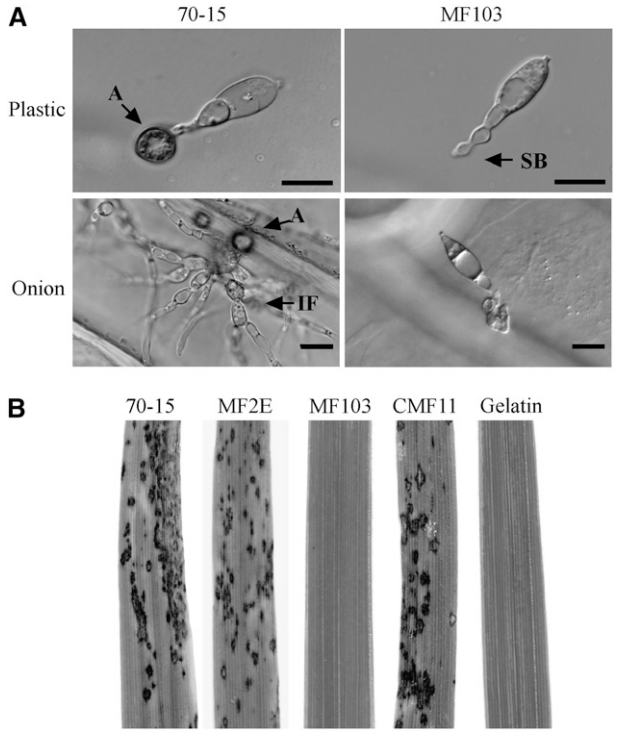

Figure 1. The *mst50* Gene Replacement Mutant.

(A) The wild-type strain (70-15) formed melanized appressoria and differentiated into infectious hyphae in onion epidermal cells. The *mst50* mutant (MF103) failed to form appressoria but produced swollen bodies along germ tubes. Images were taken 24 h after inoculation on plastic cover slips and 48 h after inoculation on onion epidermis. A, appressorium; IF, infectious hyphae; SB, apical or subapical swollen bodies. Bars = 10 μm.

(B) Two-week-old rice seedling were sprayed with conidia of the wild-type stain (70-15), an ectopic transformant (MF2E), the *mst50* deletion mutant (MF103), or the complemented transformant (CMF11) and 0.2% gelatin solution (gelatin). MF103 failed to cause lesions on infected rice leaves.

hydrophobic surfaces. At 24 h, only ~25% of RD1 germ tubes developed appressoria (Table 3, Figure 2C). Under the same conditions, >90% of germ tubes formed appressoria in 70-15 and CMF11. Interestingly, we observed that exogenous cAMP stimulated appressorium formation in RD1. When 10 mM cAMP was added to the conidial suspension (Table 3), >40% of the RD1 germ tubes formed appressoria (Table 3). In the *mst50* mutant MF103 and transformant SD1, addition of 10 mM cAMP failed to induce appressorium formation (Table 3). These data suggest that expressing the *MST50*$^{\Delta RAD}$ allele only partially rescued the defect of the *mst50* mutant in appressorium formation.

We also observed that the number of lesions that developed on leaves sprayed with RD1 was <30% of those on leaves inoculated with the wild-type strain 70-15 (Table 3), indicating that the virulence of transformant RD1 was reduced. Although the RAD domain of *MST50* is not essential for appressorium formation and plant infection, it must be required for full virulence in *M. grisea*. When assayed for the intracellular cAMP level in mycelia, we found that transformant RD1 had a higher level than that of 70-15 (Table 4). Therefore, *MST50* may be involved in interacting with components of the cAMP signaling pathway via its RAD. Reduced appressorium formation and virulence in transformant RD1 may be related to its defect in the cAMP signaling pathway.

SAM but Not RAD Is Essential for the Interaction of Mst50 with Mst11

Mst50 is known to interact with the MEKK Mst11 and the MEK Mst7 in *M. grisea* (Zhao et al., 2005). To determine the role of the SAM and RAD domains in the interaction of Mst50 with Mst11 and Mst7, we generated the bait and prey constructs of Mst50-SAM (SAM deletion) and Mst50-RAD (RAD deletion). In yeast two-hybrid assays, no detectable interaction was observed between Mst50-SAM and Mst11 (Figure 3A). However, Mst50-RAD still strongly interacted with Mst11 (Figure 3A), indicating that SAM but not RAD of Mst50 is involved in the interaction with Mst11. We also assayed the interaction of Mst7 with Mst50-SAM and Mst50-RAD. Both Mst50-SAM and Mst50-RAD still interacted with Mst7 (Figure 3B), indicating SAM and RAD were dispensable for the Mst50–Mst7 interaction. However, no detectable interaction between the middle region of Mst50 (residues

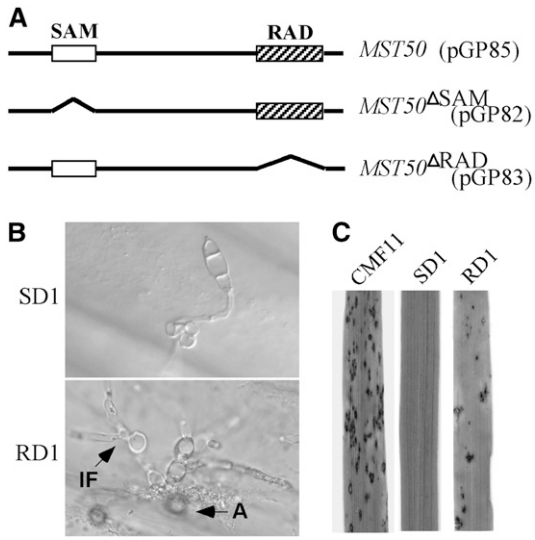

Figure 2. *MST50* Mutant Alleles Deleted from SAM or RAD.

(A) SAM (residues 67 to 130; open box) and RAD (residues 370 to 456; hatched box) of *MST50* were deleted in the *MST50*$^{\Delta SAM}$ (pGP82) and *MST50*$^{\Delta RAD}$ (pGP83) constructs, respectively. Both pGP82 and pGP83 had the *MST50* native promoter and terminator sequences as pGP85 and were transformed into the *mst50* mutant MF103.

(B) Appressorium formation and penetration assays on onion epidermis with MF103 transformants expressing the *MST50*$^{\Delta SAM}$ (RD1) and *MST50*$^{\Delta RAD}$ (SD1) alleles. A, appressorium; IF, infectious hyphae.

(C) Rice leaves were sprayed with conidial suspensions of CMF11 expressing the wild-type *MST50*, SD1, and RD1. Leaves inoculated with SD1 had fewer lesions than those inoculated with CMF11, but RD1 failed to cause any lesions under the same conditions.

Table 3. Effects of Deleting the SAM and RAD Domains of *MST50* on Plant Infection

Strain	Appressorium Formation (%)[a]		Lesion Formation (Lesions/5-cm Leaf Tip)[b]
	0 cAMP	10 mM cAMP	
70-15	95.0 ± 2.3	89.4 ± 3.2	12.3 ± 3.6
SD1	0	0	0
RD1	20.0 ± 3.0	36.7 ± 5.4	3.7 ± 1.6
MF103	0	0	0

[a] Percentage of germ tubes forming appressoria by 24 h on hydrophobic surfaces. Means and standard errors were calculated from three independent experiments (at least 100 germ tubes were examined in each repeat).
[b] Lesion formation was examined on infected rice leaves 7 DAI.

131 to 367) and Mst7 was observed in yeast two-hybrid assays (Figure 3B). Therefore, the exact Mst7-interacting site on Mst50 is not clear.

Expression of a Dominant Active *MST7* Allele Partially Rescues the Defect of the *mst50* Mutant

The dominant active *MST7*$^{S212D\ T216E}$ construct pHZ18 (Zhao et al., 2005) was transformed into the *mst*50 mutant MF103. MA7-5 (Table 1) was one of the four transformants carrying a single copy of ectopically integrated pHZ18. On plastic cover slips and onion epidermal cells, MA7-5 germlings formed melanized appressoria (Figure 4A). However, appressoria formed by MA7-5 failed to penetrate onion epidermal cells and develop infectious hyphae (Figure 4A). No lesions were formed on rice leaves inoculated with conidia of MA7-5 (Figure 4B). As a control, we transformed the wild-type *MST7* gene into MF103 and isolated eight transformants harboring pHZ10 (Zhao et al., 2005), including MW15 (Table 1). All of these transformants were phenotypically similar to the *mst50* mutant and failed to form appressoria or infect rice plants (Figure 4). These data indicate that expressing the *MST7*$^{S212D\ T216E}$ allele, but not the wild-type *MST7*, rescues the defects of the *mst50* deletion mutant in appressorium formation. However, similar to transformants of the *mst7* mutant expressing *MST7*$^{S212D\ T216E}$ (Zhao et al., 2005), MA7-5 was still defective in appressorial penetration and nonpathogenic.

To confirm that Pmk1 was activated by expressing the dominant active *MST7* in the *mst50* mutant, we assayed TEY phosphorylation of Pmk1 with an anti-TpEY–specific antibody. In total proteins extracted from the *mst50* mutant MF103 and transformant MW15, the Pmk1 (42-kD) band was not detectable by the anti-TpEY–specific antibody (Figure 4C). In MA7-5 and the wild-type 70-15, TEY phosphorylation of the Pmk1 MAP kinase was detectable in vegetative hyphae harvested from complete medium (CM) cultures (Figure 4C). These data indicate that *MST50* functions upstream from Mst7 and Pmk1 in *M. grisea*.

Mst50 Is Highly Expressed in Appressoria

To determine the expression pattern and localization of *MST50*, we generated the Mst50-enhanced green fluorescent protein (EGFP) fusion construct pHZ64. After transforming pHZ64 into MF103, zeocin-resistant transformants carrying a single copy of pHZ64, including MHZ8 and MHZ13 (Table 1), were isolated. All these transformants formed appressoria as efficiently as the wild-type strain and were fully pathogenic on rice plants. By protein gel blot analysis, a band of the expected Mst50-EGFP fusion size was detectable in MHZ8 and MHZ13 with an anti-GFP antibody (data not shown). In all these transformants, however, no or very weak GFP signal was detectable in vegetative hyphae (Figure 5A), indicating that *MST50* was expressed in mycelia but its expression level was low. Conidia and germ tubes exhibited only weak GFP signals (Figures 5A and 5B). During appressorium formation, however, GFP signals were enhanced in young and mature appressoria (Figure 5). In contrast with transformants expressing GFP-Pmk1 (Bruno et al., 2004), nuclear localization of GFP signals was not observed in MHZ8 and MHZ13. In infectious hyphae that formed inside onion epidermal cells, GFP signals were also detectable (Figure 5B). At 72 h, only appressoria that had not penetrated retained GFP signals (Figure 5B). These data suggest that *MST50* is constitutively expressed in *M. grisea* at a relatively low level but its expression was enhanced during appressorium formation and penetration.

Coimmunoprecipitation of Mst7 or Mst11 with Mst50

To further prove that Mst50 interacts with Mst7 and Mst11, we generated Mst50-6His (pHZ91), Mst7-GFP (pHZ60), and Mst11-HA (pYK63) fusion constructs and transformed them in pairs (pHZ91+pHZ60 or pHZ91+pYK63) into the wild-type strain 70-15. The resulting transformants resistant to both hygromycin and bleomycin were screened by PCR and analyzed by DNA gel blot hybridizations. Transformants M7-1 and H11-8 (Table 1) were confirmed to contain transforming vectors pHZ91 and pHZ60, and pHZ91 and pYK63, respectively. In total proteins isolated from developing appressoria and proteins eluted from Ni-NTA HisBind resins, both the 52-kD Mst50-6His and 85-kD Mst7-GFP fusion proteins were detected with anti-His and anti-GFP antibodies, respectively, in transformant M7-1 (Figure 6A). In the control experiment, the anti-actin antibody detected 45-kD actin only in total proteins but not in proteins eluted from Ni-NTA HisBind resins. These data indicate that the Mst7-GFP fusion was pulled down with Mst50-6His by Ni-NTA HisBind resins. In transformant H11-8, we were able to detect both Mst50-6His

Table 4. Measurement of Intracellular cAMP Levels in Mycelia

Strain	fmol of cAMP/mg of Mycelia[a]	70-15 (%; Wild Type)
70-15	4503.4 ± 383.2[b]	100.0
SD1	3562.3 ± 453.8	79.1
RD1	6442.4 ± 54.0	143.1
MF103	4194.7 ± 271.2	93.1
MRD	3296.3 ± 152.9	73.2
DA128	1353.0 ± 87.2	30.0

[a] Lyophilized weights of mycelia.
[b] Means and standard errors were calculated from three independent experiments.

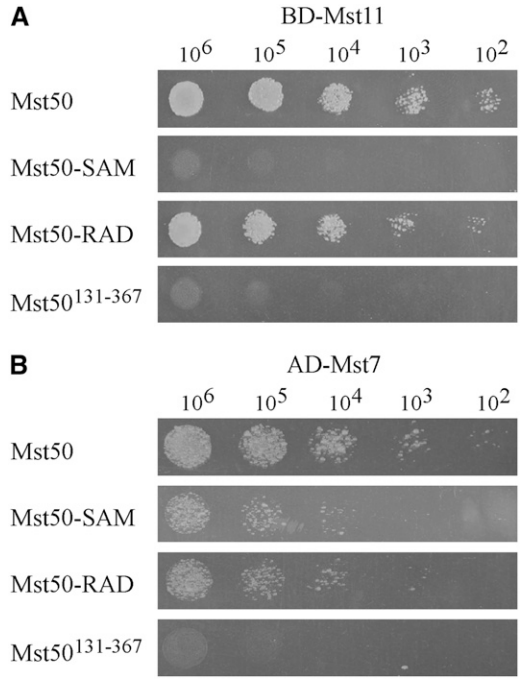

Figure 3. SAM and RAD Domains Play Different Roles in the Interaction of Mst50 with Mst11 and Mst7.

The full-length Mst50, Mst50-SAM (SAM deletion), Mst50-RAD (RAD deletion), and Mst50$^{131-367}$ (the Mst50 middle region; residues 131 to 167) constructs were assayed for their interactions with the Mst11 bait **(A)** and Mst7 prey constructs **(B)**. The resulting yeast transformants were assayed for growth on SD-Leu-Trp-His plates at specified concentrations (cells/mL).

and Mst11-HA fusions in proteins eluted from Ni-NTA HisBind resins. In proteins isolated from the wild-type strain, the Mst50-6His, Mst7-GFP, and Mst11-HA fusion proteins were not detected (Figure 6). These data indicate that Mst50 interacts with both Mst11 and Mst7 in *M. grisea* during appressorium formation.

Mst50 Interacts with Ras1 and Ras2

Since Mst50 has a RAD domain, we assayed the interaction of Mst50 with two predicted Ras homologs in *M. grisea*, Ras1 (MG09499) and Ras2 (MG06154). In yeast two-hybrid assays, both Ras1 and Ras2 directly interacted with Mst50 (Figure 7). No significant difference in the strength of the interaction between Mst50 and Ras1 or Ras2 was observed. We also examined the effect of RAD deletion on the interaction of Mst50 with Ras1 and Ras2. Deletion of the RAD domain eliminated the interaction of Mst50 with Ras1 or Ras2 in yeast two-hybrid assays (Figure 7). These data indicate that RAD of Mst50 is essential for binding to Ras1 or Ras2 and likely the binding site for Ras1 and Ras2. We introduced the G23V mutation to the Ras2 yeast two-hybrid bait vector pCX69. In yeast two-hybrid assays, no significant difference was observed between the interaction of Mst50 with Ras2 and Ras2^{G23V}, suggesting that the activated form of Ras2 may have no obvious effect on its interaction with Mst50.

Mst50 May Function Downstream from Ras Signaling in *M. grisea*

The *RAS1* and *RAS2* gene replacement constructs were generated by ligation-PCR and transformed into wild-type 70-15. The *ras1* deletion mutant MCX77 (Table 1) still formed appressoria and was pathogenic on rice plants. No obvious defect other than a reduction in conidiation was observed in MCX77. We were unable to identify a *ras2* deletion mutant. These data indicate that

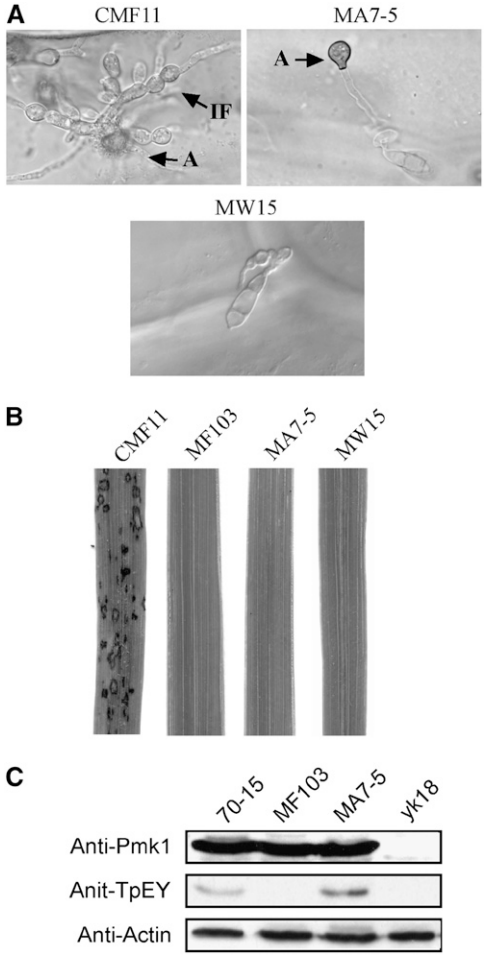

Figure 4. Expression of a Dominant Active *MST7* Allele in the *mst50* Mutant.

(A) Appressorial penetration assays with transformants of mutant MF103 expressing wild-type *MST50* (CMF11), dominant active *MST7*$^{S212D\ T216E}$ (MA7-5), or wild-type *MST7* (MW15). Although melanized appressoria were formed by MA7-5, only CMF11 penetrated onion epidermal cells. A, appressorium; IF, infectious hyphae.

(B) Rice leaves were sprayed with conidia from CMF11, MF103, MA7-5, and MW15. Blast lesions were observed only on leaves sprayed with CMF11.

(C) Total proteins were isolated from mycelia of 70-15, MF103, MA7-5, and the *pmk1* mutant yk18. The anti-Pmk1 antiserum detected a 42-kD Pmk1 band in all the samples except yk18. An anti-Phopho 42/44 antibody (anti-TpEY) detected a 42-kD band only in 70-15 and MA7-5. Detection with an anti-actin antibody was the control.

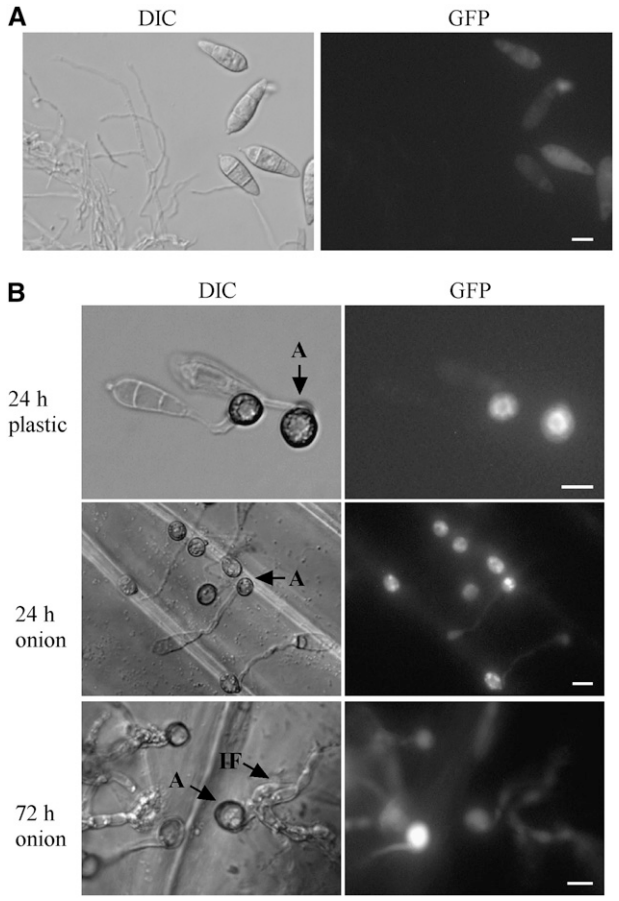

Figure 5. Analysis of the Expression of a *MST50*-GFP Fusion Construct.

(A) Conidia and vegetative hyphae of MHZ8 examined with differential interference contrast (DIC) or epifluorescence microscopy (GFP).

(B) Appressoria formed by MHZ8 on plastic cover slips or onion epidermis were examined by differential interference contrast (DIC) or epifluorescence microscopy (GFP). At 24 h, most appressoria had strong fluorescence, but only appressoria that did not penetrate retained fluorescence at 72 h. Weak GFP signals were observed in conidia, germ tubes, and infectious hyphae. A, appressorium; IF, infectious hyphae. Bars = 10 μm.

RAS1 and *RAS2* have distinct functions in *M. grisea. RAS1* is dispensable for fungal growth and plant infection. By contrast, *RAS2* may be an essential gene and play a more critical role than *RAS1* in *M. grisea*.

To determine the relationship between *MST50* and *RAS2*, we constructed a dominant active *RAS2* allele (pCX66) by changing the highly conserved Gly-23 to Val (Barbacid, 1987; Ha et al., 2003). After transforming pCX66 into the wild-type strain 70-15 and the *mst50* deletion mutant MF103, zeocin-resistant transformants were isolated and analyzed by DNA gel blot hybridization. MCX66 and MHZ66 were transformants of 70-15 and MF103, respectively, which contained a single copy of pCX66. Conidia produced by MCX66 formed melanized appressoria efficiently on both hydrophobic and hydrophilic surfaces. However, the morphology and size of appressoria formed by MCX66 varied significantly (Figure 8). Some appressoria of MCX66 were formed on branching germ tubes or at intercalary positions. By contrast, no appressorium was formed by MHZ66 (Figure 8). These data indicate that the expression of the *RAS2*^{G23V} allele in the wild type but not the *mst50* mutant may lead to improper activation of the Pmk1 pathway and stimulate abnormal appressorium formation. We also transformed pCX66 into the *pmk1* mutant nn78. The expression of *RAS2*^{G23V} in transformant MRN78 (Table 1) failed to induce appressorium formation. Similar to MRN78, transformants of the *mst7* and *mst11* mutants expressing *RAS2*^{G23V} failed to form appressoria on hydrophobic surfaces, indicating that deletion of *MST50*, *MST11*, *MST7*, or *PMK1* abolished the dominant effect of Ras2^{G23V} on appressorium formation. Therefore, it is likely that *RAS2* functions upstream from *MST50* in activating the Pmk1 MAP kinase cascade.

To further prove that the dominant activity of Ras2 is responsible for stimulating appressorium formation in MCX66, we generated a *RAS2*^{G23V} construct deleted from the RAAS box (residues CVLM). In transformant MCX90 (Table 1) expressing the *RAS2*$^{G23V\ \Delta CAAX}$ construct, normal melanized appressoria were formed on hydrophobic surfaces (Figure 8B) but not on hydrophilic surfaces (data not shown), indicating that deletion of the CAAX box eliminated the dominant activity of *RAS2*^{G23V}. We also introduced the putative dominant negative *RAS2*^{S28N} and DN CtRas (Ha et al., 2003) constructs into 70-15. The resulting transformants had no obvious phenotypic changes in appressorium formation and plant infection. Even in transformant MCX99 (Table 1) expressing the RP27-*RAS2*^{S28N} construct, appressorium formation was not affected. Therefore, the S28N mutation may lack the putative dominant effect or have no gain-of-function activities in *M. grisea*.

Mst50 Directly Interacts with Mgb1 and MgCdc42 in Yeast Two-Hybrid Assays

In *M. grisea*, the Mgb1 Gβ subunit has been implicated in appressorial penetration and may function upstream from the Pmk1 MAP kinase pathway (Nishimura et al., 2003). In yeast two-hybrid assays, Mst50 strongly interacted with the Gβ subunit Mgb1 (see Supplemental Figure 1 online). For the Mst50–Mgb1 interaction, both SAM and RAD of Mst50 were dispensable (data not shown). We also assayed the interaction of Mst50 with a predicted Cdc42 homolog in *M. grisea* MgCdc42 (see Supplemental Figure 1 online). The Mst50–MgCdc42 interaction was as strong as the interaction between Mst50 and Mgb1. These yeast-two hybrid data suggest that *MST50* may interact with multiple upstream factors that are involved in the activation of the *PMK1* MAP kinase pathway in *M. grisea*.

MST50 Is Involved in Regulating Cell Wall Integrity and Osmoregulation

We assayed the *mst50* mutant for the cell wall defect and sensitivity to hyperosmotic stresses. Vegetative hyphae of the *mst50* mutant MF103 released abundant protoplasts after 20 min of digestion with cell wall lytic enzymes (see Supplemental Figure 2 online). Under the same conditions, mycelia of 70-15 produced only a few protoplasts, indicating that the *mst50* mutant, similar

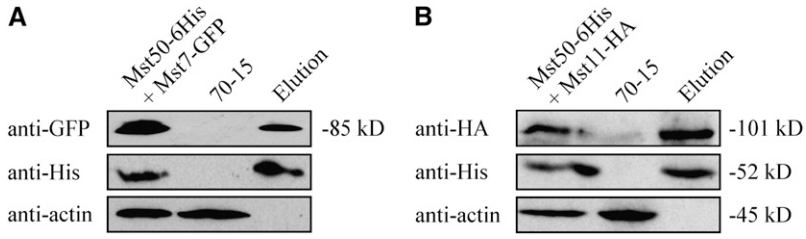

Figure 6. Coimmunoprecipitation Assays of Mst7 or Mst1 with Mst50.

Protein gel blots of protein samples isolated from the wild-type strain 70-15 and transformants M7-1 **(A)** or H11-8 **(B)** were detected with the anti-HA, anti-6His, anti-GFP, or anti-actin antibody. Lanes on the left (Mst50-6His+Mst11-HA or Mst50-6His+Mst7-GFP) and right (elution) were total proteins and proteins eluted from Ni-NTA HisBind resins, respectively. The middle lane was total proteins from 70-15.

to the *mst11* mutant (Zhao et al., 2005), had weakened cell walls and was more sensitive to cell wall lytic enzymes. We also measured the growth rate on CM supplemented with Calcofluor and Congo Red (50 to 200 μg/mL) but failed to observe any significant difference between 70-15 and MF103. However, conidia and vegetative hyphae of MF103 had weaker fluorescent signals after Calcofluor staining than those of 70-15 (data not shown). In the presence of 100 μg/mL Calcofluor, only 27.1 ± 6.5% of MF103 conidia germinated by 24 h, but conidium germination in 70-15 (95.7 ± 4.2%) was not affected.

The *mst50* mutant also was more sensitive to hyperosmotic stresses. In the presence of 1 M sorbitol, the reduction of growth rate on oatmeal agar plates was more severe in MF103 than in 70-15 or MF2E (Table 2), indicating that *MST50* is also involved in osmoregulation in *M. grisea*, possibly by crosstalking with the *OSM1* pathway (Dixon et al., 1999). We also assayed colonial growth on CM and 5× YEG with 1 M sorbitol or 1.4 NaCl. In all the media tested, the *mst50* mutant was more susceptible to hyperosmotic stresses than the wild-type strain 70-15 (data not shown). Interestingly, the expression of the dominant active but not the wild-type *MST7* allele rescued the defect of the *mst50* mutant in enhanced sensitivity to hyperosmotic stresses in MF103 (Table 2).

DISCUSSION

In *M. grisea*, appressorium formation and invasive growth are regulated by the Mst11-Mst7-Pmk1 MAP kinase cascade (Xu and Hamer, 1996; Zhao et al., 2005). What activates the Mst11 MEKK is not clear, although the Mgb1 Gβ subunit has been implicated in activating the *PMK1* pathway (Nishimura et al., 2003). Mst50, a homolog of yeast Ste50, physically interacts with Mst11 and Mst7 (Zhao et al., 2005). In this study, we presented several lines of evidence to demonstrate that *MST50* functions as an upstream component of the *PMK1* pathway for regulating appressorium formation (Figure 9). First, the *mst50* and *mst11* deletion mutants had similar phenotypes, including defects in appressorium formation and plant infection and sensitivity to hyperosmotic stresses. Secondly, Mst50 physically interacted with Mst11 via the SAM domain in yeast two-hybrid assays. Deletion of SAM in Mst50 abolished its interaction with Mst11 (Figure 3) and its activity in appressorium formation (Figure 2). Our preliminary data indicated that deletion of SAM in Mst11 also eliminated the Mst50–Mst11 interaction. In addition, we found that expressing a constitutive active but not the wild-type *MST7* allele restored appressorium formation in the *mst50* mutant. These data indicate that *MST50* plays an essential role in the activation of the Mst11-Mst7-Pmk1 cascade.

In *S. cerevisiae*, Ste50 acts as an adaptor protein sustaining and facilitating signal transduction between activated G proteins and MAP kinase cascades, but it is not an indispensable upstream factor for activating MAP kinase cascades (Ramezani-Rad, 2003). Deletion of *STE50* results in a reduction in mating and filamentous growth, and these defects can be complemented by overexpressing *STE11* (Rad et al., 1998; Jansen et al., 2001). In *M. grisea*, Mst50 is essential for activating the Pmk1 MAP kinase cascade. Similar to mutants blocked in several key components of the *PMK1* pathway (Xu and Hamer, 1996; Nishimura et al., 2003; Zhao et al., 2005), the *mst50* deletion mutant was nonpathogenic and failed to form appressoria. The function of Mst50 in activating the downstream Pmk1 cascade is more similar to that of Ste4 in *S. pombe* and Ubc2 in *U. maydis*. Both Ste4 and Ubc2 are homologs of Ste50 required for activating the homologous MAP kinase cascade. The *ubc2* deletion mutant is nonpathogenic and defective in conjugation tube formation (Mayorga and Gold, 2001). In contrast with other Ste50 homologs,

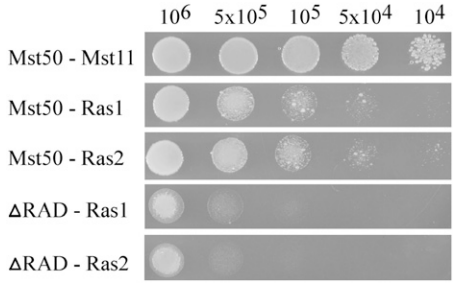

Figure 7. Yeast Two-Hybrid Assays of the Interaction between Mst50 and Ras1 or Ras2.

The full-length Mst50 (top three rows) and Mst50-RAD (bottom two rows) were used as the bait. Ras1 and Ras2 were used as the prey. The Mst50-Mst11 interaction was used as the positive control. Yeast cells grown on SD-Leu-Trp were diluted to specified concentrations (cells/mL) and plated onto SD-Leu-Trp-His for examining the expression of the *HIS3* reporter gene.

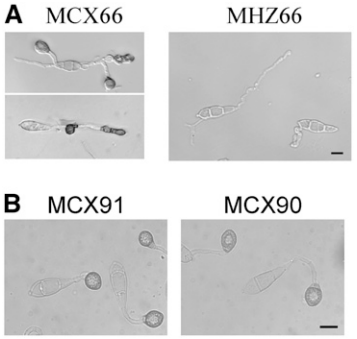

Figure 8. Appressorium Formation Assays on Plastic Cover Slips.

(A) Expression of a dominant active *RAS2* allele in the wild-type 70-15 (MCX66) and the *mst50* mutant MF103 (MHZ66). Transformant MCX66 formed melanized appressoria with abnormal morphology and positions on hydrophobic plastic cover slips. Under the same conditions, MHZ66 failed to form any appressorium.

(B) Expression of a putative dominant negative *RAS2* allele (MCX91) and the $Ras2^{G23V\ \Delta CAAX}$ (MCX90) in 70-15 had no effect on appressorium formation. Normal melanized appressoria were efficiently formed by transformants MCX91 and MCX90.

Ste4 has a leucine zipper motif and may function as a putative transcription factor. The *ste4* mutant in *S. pombe* is sterile (Okazaki et al., 1991; Barr et al., 1996).

Mst50 and Mst11 directly interact with each other, and both of them have the SAM and RAD domains (Zhao et al., 2005). Our results indicate that SAM mediates the Mst50–Mst11 interaction that is essential for regulating infection-related morphogenesis in *M. grisea*. The SAM domain is known to mediate protein–protein interaction or RNA binding (Kim and Bowie, 2003; Johnson and Donaldson, 2006). It is present in a variety of proteins involved in signal transduction or transcriptional activation and repression. In the *M. grisea* genome, Mst11, Mst50, and MG06334 are the only SAM-containing genes. The role of SAM domains in Ste50 and Ste11 interaction are well characterized in *S. cerevisiae* (Bhattacharjya et al., 2004; Kwan et al., 2006). The association between the homologs of Ste11 and Ste50 also has been reported in *S. pombe* and *U. maydis* (Barr et al., 1996; Mayorga and Gold, 2001). In contrast with the Mst50–Mst11 association, the direct interaction between Mst50 and Mst7 was a unique phenomenon in *M. grisea*. In yeast, Ste50 does not interact with Ste7 in yeast two-hybrid assays (Xu et al., 1996). In *U. maydis*, no direct interaction between Ubc2 and Ubc4/Fuz7 was observed (Mayorga and Gold, 2001). Our yeast two-hybrid data suggest that both SAM and RAS of Mst50 are not essential for the interaction with Mst7. However, the middle region between SAM and RAD alone is not sufficient for interacting with Mst7. Therefore, the exact Mst7-interacting site on Mst50 is not clear. The middle region of Mst50 is well conserved among filamentous ascomycetes, but it has no known motif or domain. To date, no Ste50 homolog has been functionally characterized in filamentous ascomycetes. Although SAM and RAD are not essential for the Mst50–Mst7 interaction, it is possible that the association of Mst50 with Mst7 requires either SAM or RAD to maintain certain structures or configurations. Deletion of both SAM and RAD may adversely affect the structure of Mst50 and abolish the Mst50–Mst7 interaction.

Mst50 has the RAD and it directly interacts with Ras1 and Ras2 of *M. grisea*. In *S. cerevisiae*, the RAD of Ste50 is required for its interaction with Ras2 in yeast two-hybrid assays and for mating, invasive growth, and high-osmolarity glycerol response signaling in vivo (Ramezani-Rad, 2003; Truckses et al., 2006). In the *M. grisea* genome, Mst11, Mst11, and the Mac1 adenylate cyclase (Adachi and Hamer, 1998) are the only predicted proteins with a RAD domain identified. The RAD was first identified in Ras/Rap1 effectors, including guanine-nucleotide releasing factor in mammals (Ponting and Benjamin, 1996). However, RAD sequences also are present in a number of other proteins, including the adenylate cyclase and Ste50 in *S. cerevisiae* (Kido et al., 2002; Ramezani-Rad, 2003). Ras homologs are known to regulate the cAMP-protein kinase A (PKA) pathway and filamentous growth in *S. cerevisiae* (Rudoni et al., 2001; Wang et al., 2004) and mating processes in *S. pombe* (Papadaki et al., 2002). Ras signaling has also been implicated in various infection and morphogenetic processes in several fungal pathogens, including *U. maydis* (Lee and Kronstad, 2002; Muller et al., 2003), *Colletotrichum trifolii* (Chen and Dickman, 2005), and *Cryptococcus neoformans* (Waugh et al., 2002). In *M. grisea*, *RAS2* appears to be an essential gene. Expressing the dominant active allele of *RAS2* in the wild type (Figure 8) but not in the *mst50*, *pmk1*, *mst7*, or *mst11* mutant stimulated inappropriate appressorium formation, indicating that *MST50*, *MST11*, *MST7*, or *PMK1* is required for $Ras2^{G23V}$ to exhibit a dominant effect on appressorium formation. Although the interaction between Ras2 and Mst50 was not affected by the

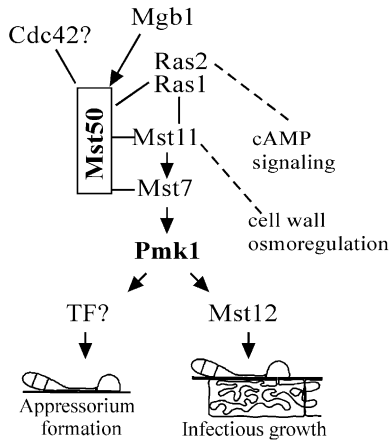

Figure 9. Hypothetical Model for the Functions of Mst50 in *M. grisea*.

Mst11 and Mst7 are the MEKK and MEK that activate Pmk1. Mst50 interacts with both Mst11 and Mst7 and may function as the adaptor protein for the Pmk1 MAP kinase pathway. The Gβ subunit Mgb1, a Cdc42 homolog, and Ras proteins Ras1 and Ras2 all directly interact with Mst50. These proteins may be responsible for transducing various upstream signals to activate the Mst11-Mst7-Pmk1 cascade for regulating different plant infection processes via the Mst12 and other transcription factors (TFs). Mst50 and Mst11 are likely involved in crosstalking with the cell wall integrity and osmoregulation pathways. Ras2 may function above the cAMP signaling pathway that regulates surface recognition and appressorium initiation.

Table 5. PCR Primers Used in This Study

Name	Sequence (5′→3′)
N6	ATAGTTATGCGGCCGCCGCCTTTCCATTGGAAG
B5	CGCGGATCCGGAGGATCTCGACTTTGT
C3	CCCATCGATAGGAAGGAATAGCGGGAA
X1	CCGCTCGAGAAGAGCTGTAGCGTCACGTA
KF1	TATCTCAACCGACGCGTT
KR2	ACCTATTTGAGCAGGACT
S1F	CTATAGGGCGAATTGGGTACTCAAATTGGTTGGATACTCTGGTATCTTCGT
S2R	CCGAGAAACTAGGCCAGCAGTAGACACTTGGAAGAGCTGTAGCGTCACGTA
GBF1	CCGGAATTCATGGATTCACAACGGTCA
GBR2	ATTGGTTCTGCAGTTTAGTATGCCCAGATCTT
BF1	CTGGAATTCATGGCTCAGTCAAAGGTTCGTC
BR1	CTGCTGCAGTTACATCAAGACACACTTGGAG
BF7	GATCGCTAGCATGACTGGAAGGTTGCAGCTCCAC
BR7	GATCCTGCAGTCACAATATAACACACTTGATCG
F29	CCGGAATTCGAGACAATCATCAAGGCGCAGGACGTGCCGGTGGAGA
R30	CCAATGCATTGGTTCTGCAGCTCATATTATTCCTCCTGGGGGATCAT
F9	GATCGGAATTCATGAGCTTCAACACGGGGACGGCGTA
R31	CCAATGCATTGGTTCTGCAGCTCATGGCGTCTGCATCCTGCG
SF20	CTATAGGGCGAATTGGGTACTCAAATTGGTTGGATACTCTGGTATCTTCGT
SR22	TGGTCGCTCTCCACCGGCACGTCCTGCGCCTTGATGATTGTCTCCGGTAGGCGA
SF21	ATCGCCTACCGGAGACAATCATCAAGGCGCAGGACGTGCCGGTGGAGAGCGACC
SR24	TTCCCGCTATTCCTTCCTACTTGATTCATATTATTCCTCCTGGGGGATCA
SF23	TGATCCCCCAGGAGGAATAATATGACTCAAGTAGGAAGGAATAGCGGGAA
SR19	CCGAGAAACTAGGCCAGCAGTAGACACTTGGAAGAGCTGTAGCGTCACGTA
SR15	ATGGGCGAGCTGTCGTGAATGTCCCTCTCGTACTCGTCGTCTGCGTCCGA
SF16	ATGAGCTTCAACACGGGGACGGCGTACGCCGAGTCGGACGCAGACGACGA
SR17	TGCCTGGCGCCTCGTTGCCAATGTCAACCTGCGCATTTGGCGTCTGCATCCTGCGCGGCGCCA
SF18	TGGCGCCGCGCAGGATGCAGACGCCAAATGCGCAGGTTGACATTGGCAACGAGGCGCCAGGCA
50GF	CGACTCACTATAGGGCGAATTGGGTACTCAAATTGGTGGACCATACTTCAACCTACTCA
50GR	CACCACCCCGGTGAACAGCTCCTCGCCCTTGCTCACTATTATTCCTCCTGGGGGA
CDC1F	CCGGAATTCCTCCAAACAATGGTGGTTGCA
CDC2R	CCGCTCGAGTCAAAGGATCAGGCACTTTT
RASUF	CATGGGCCCGCAGCGTCCTATCACTACTACC
RASUR	GATCGATCGGAGGGCTTCTTTCGT
RASGF	GTTGTCGGCGGCGTCGGTGTC
RASGR	GACACCGACGCCGCCGACAAC
RS1F1	GATCGGATCCCGCCTACGACCCATGTCGAAGAG
RS1R1	GATCAGGCGCGCCATTGTGCCCTTCCTTGGTTTGC
RS1F2	CGATCGGCCGGCCTCGATGGCCACCGCTTGACTC
RS1R2	GTCACCAAGGACTACCAAGCTTTCTCAC
RS2F1	GGTCCTGCAGCGAGGAAGGTCGATACCTCACTC
RS2R1	GTCAGGCGCGCCGTGGAATTCGATCGCTTCTCTC
RS2F2	GTCAGGCCGGCCGTGCTGCTCCAAGTGTGTCTTG
RS2R2	GTCAGCGGCCGCCACCAGAAACGAGGACAACAGC
50DDP	CGACTCACTATAGGGCGAATTGGGTACTCAAATTGGTGGACCATACTTCAACCTACTCA
50Hi	GGTGAACAGCTCCTCGCCCTTGCTCACTCAATGGTGATGGTGATGGTGAGCAGCAGCTATTATTCCTCCTGGGGGA
M7GFP	CGACTCACTATAGGGCGAATTGGGTACTCAAATTGGTGAGAGGAGCACGACAGATCT
M7GRP	CACCACCCCGGTGAACAGCTCCTCGCCCTTGCTCACGAAACCATAACTCCCAGTCGA
50MCF	AATAGAATTCAAGGCGCAGGACGTGCCGGTGGAGA
50MCR	ATAACTCGAGCTGCATCCTGCGCGGCGCCACCGGCT
NSF1	CCATCGATTCCGTGCAGTCCTTGC
HAS11R	GCACTAGTTTAAGCGTAATCTGGAACATCGTATGGGTACGTGATAGGAGTCAG
RASdaf	CTGGTGGTTGTCGGCGGCGTCGGTGTCGGTAAATCATGC
RASdar	GCATGATTTACCGACACCGACGCCGCCGACAACCACCAG

G23V mutant, our preliminary data indicated that the Ras2–Mst11 interaction was significantly enhanced by this dominant active mutation in Ras2 mutation. The enhanced Mst11-Ras2^{G23V} interaction may be responsible for activating the Pmk1 MAP kinase cascade for appressorium formation in transformants expressing *RAS2*^{G23V}. Therefore, it is likely that Ras2 functions upstream from Mst50 in activating the Pmk1 MAP kinase cascade in *M. grisea*. In *S. pombe*, both Ste4 and Ras1 function upstream of Byr2 and act at least partially independently (Tu et al., 1997). Since expressing a *MST50*$^{\Delta RAD}$ allele could partially complement the defect of the *mst50* mutant in appressorium formation and virulence on rice seedlings, the association of Mst50 with Ras2 may not be essential for appressorium formation. However, Mst11 interacts with Mst50, and it also has the RAD domain. Association between Mst11 and Ras2 may bring Ras2 and Mst50 together in the strain containing *MST50*$^{\Delta RAD}$ and result in weak activation of the downstream Pmk1 MAP cascade.

Our yeast two-hybrid data indicate that Mst50 may also interact with Mgb1 and the Cdc42 homolog in *M. grisea*. The *MGB1* gene is essential for appressorium formation and appressorial penetration (Nishimura et al., 2003), but the Mg *CDC42* deletion mutant still formed melanized appressoria and caused small lesions on rice plants (S. Wu and Z. Wang, personal communication). In *S. cerevisiae*, *CDC42*, *STE20*, *STE50*, and *STE11* are shared components in MAP kinase pathways regulating mating, filamentous growth, and osmotolerance. Cdc42 interacts with both Ste50 and the p21-activated protein kinase Ste20. The association with Cdc42 is responsible for bringing Ste20 together with the Ste11-Ste50 complex to activate Ste11 (Ramezani-Rad, 2003). In *M. grisea*, however, the mutant deleted from the *STE20* homolog had no obvious defect in plant infection and in responses to osmotic stresses (Li et al., 2004). Although the Cdc42 homolog interacts with Mst50, its role in *M. grisea* must be different from linking a p21-activated protein kinase to the activation of Mst11.

Mst50 appears to bind to different components of the *PMK1* MAP kinase pathway and function as an adaptor protein. In contrast with Ubc2 (Mayorga and Gold, 2001), Mst50 and its homologs from other filamentous ascomycetes lack C-terminal Src Homology 3 domains that are involved in protein–protein interactions. It will be important to identify and characterize the binding sites of Mst50 for different proteins, such as Mgb1 and Mst7. *MST50* may function as the adaptor protein and directly mediate signal transductions between the receptor-activated heterotrimeric or monomeric G proteins (e.g., Mgb1 or Ras2) and the downstream MAP kinase cascades. However, protein(s) other than Mst50 may be involved in associating with and activating the MAP kinase cascade in response to different signals. In *S. cerevisiae*, Ste5 is the scaffold protein that interacts with different components of the pheromone response pathway (Park et al., 2003; Ptashne and Gann, 2003), but the *M. grisea* genome does not have an Ste5 homolog (Dean et al., 2005).

Exogenous cAMP stimulated appressorium formation in the MF103 transformant expressing the *MST50* $^{\Delta RAD}$ allele (Table 3). Interestingly, transformant RD1 had an elevated instead of reduced intracellular cAMP level. By contrast, transformant MRD (Table 1) expressing *MST11*$^{\Delta RAD}$ (Zhao et al., 2005) had a reduced level of intracellular cAMP (Table 4). These results were puzzling because MRD was normal in appressorium formation (Zhao et al., 2005). One possible explanation is that elevated intracellular cAMP levels are harmful to *M. grisea*, and transformant RD1 may be somewhat reduced in its sensitivity to cAMP and efficiency in cAMP signaling for appressorium initiation. RD1 still responded to exogenous cAMP because 10 mM is much higher than normal intracellular cAMP levels in *M. grisea*. In *S. cerevisiae*, Ste50 interacts with Ras2 via RAD and is involved in the PKA-dependent signal transduction pathway for controlling pseudohyphal and invasive growth (Pan and Heitman, 2002; Ramezani-Rad, 2003). RAD of Mst50 is involved in the interaction with Ras1 and Ras2 in *M. grisea* (Figure 7). However, the functions of *RAS1* and *RAS2* in cAMP signaling are not defined in *M. grisea*. The *M. grisea ras1* mutant still formed appressoria and was pathogenic on rice plants, but we were unable to isolate a *ras2* deletion mutant. Further characterization of Ras1 and Ras2 is necessary to determine the function of Mst50 in the cAMP-PKA signaling pathway, which is known to regulate surface recognition and appressorium initiation in *M. grisea* (Lee and Dean, 1993; Dean, 1997).

METHODS

Strains, Plasmids, and Growth Conditions

The wild-type strains and all the transformants generated in this study (Table 1) were cultured on oatmeal agar plates at 25°C (Xue et al., 2002). Media were supplemented with 250 μg/mL hygromycin B (Calbiochem) or 100 μg/mL zeocin (Invitrogen) for selecting hygromycin-resistant and zeocin-resistant transformants, respectively. Monoconidial culture isolation, genetic crosses, and measurements of conidiation and growth rate were performed as previously described (Li et al., 2004; Park et al., 2004). Intracellular cAMP was extracted from mycelia collected from 3-d-old 5× YEG (0.5% yeast extract and 1% glucose) liquid cultures as previously described (Nishimura et al., 2003) and detected with the cAMP enzyme immunoassay system (Amersham Pharmacia Biotech) following the manufacturer's instructions. Calcofluor (Sigma-Aldrich) and Congo Red (Sigma-Aldrich) were added to the final concentration of 50 to 200 μg/mL in CM agar to determine their effect on colonial growth. Plasmids pHZ18 and pHZ24 contained the wild-type *MST7* and dominant active *MST7*$^{S212D\ T216E}$, respectively (Zhao et al., 2005).

The *MST50* Gene Replacement Vector and Mutant

A 1.2-kb fragment upstream from *MST50* was amplified with primers N6 and B5 (Table 5) and cloned between the *Not*I and *Bam*HI sites on pGP18 (Zhao et al., 2005) as pGP28. In pGP18, the *hph* gene was cloned into the *Eco*RI site of pBluescript II KS+ (Stratagene). A 0.7-kb fragment downstream from *MST50* was amplified with primers C3 and X1 (Table 5) and cloned between the *Cla*I and *Xho*I sites on pGP28. The resulting *MST50* gene replacement vector pGP64 was digested with *Not*I and transformed into protoplasts of the wild-type strain 70-15 as previously described (Xu and Hamer, 1996). Hygromycin-resistant transformants were screened by PCR with primers KF1 and KR2. Putative *mst50* gene replacement mutants were further analyzed by DNA gel blot hybridizations. The complementation vector pGP85 was constructed by cloning a 4.3-kb fragment of *MST50* amplified with primers S1F and S2R (Table 5) into the bleomycin resistance vector pKB03 (Bruno et al., 2004).

Assays for Appressorium Formation, Penetration, and Plant Infection

Conidia harvested from 10-d-old oatmeal agar cultures were used for appressorium formation on plastic microscope cover slips (Fisher

Scientific) or GelBond membranes (Cambrex) as described (Xue et al., 2002; Tucker et al., 2004). Conidia were resuspended in 10 mM cAMP for assaying responsiveness to cAMP on the hydrophilic side of Gelbond (Lee and Dean, 1993). Two-week-old seedlings of the rice (*Oryza sativa*) cultivar Nipponbare and 8-d-old seedlings of the barley (*Hordeum vulgare*) cultivar Golden Promise were used for spray or injection infection assays (Park et al., 2004). Plant incubation and inoculation were performed as described (Valent and Chumley, 1991). Lesion formation was examined 7 DAI. Mean number of lesions formed on 5-cm leaf tips was determined as described previously (Talbot et al., 1993, 1996). Conidia and vegetative hyphae were stained with 10 μg/mL Calcofluor and observed as described previously (Xu and Hamer, 1996).

Yeast Two-Hybrid Assays

The HybridZap2.1 yeast two-hybrid system (Stratagene) was used to assay protein–protein interactions. The bait or prey vectors of Pmk1, Mst7, Mst11, and Mst50 were generated in the previous study (Zhao et al., 2005). ORFs of *MGB1*, *RAS1*, *RAS2*, and the *CDC42* homolog (MG00466) were amplified with primer pairs GBF1-GBR2, BF1-BR1, BF7-BR7, and CDC1F-CDC2R (Table 5), respectively. The amplified *MGB1* and *RAS1* ORFs were digested with *Eco*RI and *Pst*I and cloned into pAD-GAL4-2.1 (Stratagene) as the prey vectors pGP78 and pCX67, respectively. The prey constructs of the *Magnaporthe grisea CDC42* homolog and *RAS2* were cloned between the *Eco*RI and *Pst*I sites and the *Nhe*I and *Pst*I sites on pAD-GAL4-2, respectively. The resulting bait and prey vectors were cotransformed in pairs into yeast strain YRG-2 (Stratagene) with the alkali-cation yeast transformation kit (MP Biomedicals). The Leu^+ and Trp^+ transformants were isolated and assayed for growth on SD-Trp-Leu-His medium and galactosidase activities following the instructions provided by Stratagene.

To generate the Mst50-SAM (deleted from amino acids 1 to 130) construct, the *MST50* ORF was amplified from first-strand cDNA of wild-type 70-15 with primers F29 and R30 (Table 5), digested with *Eco*RI and *Pst*I, and cloned into pBD-GAL4 as the bait vector pGP86 and into pAD-GAL4-2.1 as the prey vector pGP88. The bait (pGP87) and prey (pGP89) constructs of Mst50-RAD (deleted from amino acids 370 to 489) were generated with similar approaches using primers F9 and R31 (Table 5). The middle region of Mst50 (residues 131 to 367) was amplified with primers 50MCF and 50MCR and cloned into pBD-GAL4 and pAD-GAL4-2.1 as the bait (pHZ92) and prey (pHZ93) constructs, respectively. The QuickChange II site-directed mutagenesis kit (Stratagene) was used to introduce the G23V mutation to the Ras2 bait construct pCX69 with primers RASDAF and RASDAR (pHZ109). β-Galactosidase activities were quantitatively assayed with *O*-nitrophenyl-β-D-galactoside as the substrate as described (Bartel et al., 1993).

Domain Deletion Analyses in *MST50*

The $MST50^{\Delta SAM}$ and $MST50^{\Delta RAD}$ alleles deleted from amino acid residues 67 to 130 and 370 to 456, respectively, were constructed by the PCR-mediated yeast homologous recombination approach (Bourett et al., 2002; Raymond et al., 2002). For constructing the $MST50^{\Delta SAM}$ allele, primers SF20 and SR22, SF21 and SR24, and SF23 and SR19 (Table 5) were used to amplify 2.0-, 1.2-, and 0.9-kb fragments of *MST50*, respectively. The resulting PCR products were cotransformed with *Xho*I-digested pKB03 (Bruno et al., 2004) into yeast strain XK1-25 (Xu and Hamer, 1996), and Ura^+ transformants were selected. The $MST50^{\Delta SAM}$ construct pGP82 was recovered from one of these Ura^+ transformants and confirmed by sequence analysis. Primers SF20 and SR15, SF16 and SR17, and SF18 and SR19 were used to amplify 1.8-, 1.4-, and 1.0-kb fragments of *MST50* to generate the $MST50^{\Delta RAD}$ construct pGP83 with the same approach. After transforming the *mst50* mutant MF103 with pGP82 or pGP83, zeocin-resistant transformants were isolated and analyzed by DNA gel blot hybridization to confirm the integration event.

Mst50-GFP Fusion

For constructing the *MST50*-GFP fusion vector pHZ64, the entire *MST50* ORF and a 1.5-kb upstream promoter sequence were amplified with primers 50GF and 50GR (Table 5). The resulting PCR product was cloned into the bleomycin-resistant vector pKB03 (Bruno et al., 2004) by the in vivo yeast homologous recombination approach (Bourett et al., 2002; Raymond et al., 2002). Plasmid pHZ64 was confirmed by sequence analysis to carry the *MST50*-GFP in-frame fusion construct under the control of the native *MST50* promoter.

Protein Gel Blot Analysis

Total proteins were isolated from vegetative hyphae as described previously (Bruno et al., 2004). To avoid the activation of Mps1 MAP kinase by cold treatment, fresh mycelia were harvested from 2-d-old cultures grown in CM and directly used for protein extraction. Total proteins (~20 μg) were separated on an 8% SDS-PAGE gel and transferred to nitrocellulose membranes. Antigen antibody detection was performed with the ECL Supersignal System (Pierce). The anti-Pmk1 antiserum (Bruno et al., 2004) was used to detect Pmk1 expression. A monoclonal anti-GFP antibody (Sigma-Aldrich) and a monoclonal anti-actin antibody (Sigma-Aldrich) were used to detect GFP fusion and actin proteins, respectively. TEY phosphorylation of MAP kinases was detected with the PhophoPlus p44/42 MAP kinase antibody kit (Cell Signaling Technology) following the manufacturer's instructions.

Coimmunoprecipitation Assays

The Mst50-6His fusion was constructed by cloning the PCR product amplified with primers MST50Hi and MST50DPP into pDL2 as pHZ91. *MST7* was amplified with primers MST7GFP and MST7GRP and cloned into pKB04 (Bruno et al., 2004) as pHZ60. The Mst11-HA fusion construct pYK63 was constructed by cloning the PCR product amplified with primers NSF1 and HAS11R between the *Cla*I and *Spe*I sites on pYK11 (Zhao et al., 2004). Plasmids pHZ91 and pHZ60 or pYK63 were cotransformed into the wild-type strain 70-15. Total proteins were prepared from appressoria formed by transformants M7-1 (pHZ91+pHZ60) or H11-8 (pHZ91+pYK63) on plastic Petri plates for 12 h as previously described (Bruno et al., 2004) and then incubated with Ni-NTA HisBind resins (Novagen) for 2 h at 4°C on a rotary shaker (200 rpm). After washing with 1× Ni-NTA washing buffer (Novagen) three times, proteins bound to the resins were eluted with 1× Ni-NTA elution buffer. The elution was then used for protein gel blot analysis with the anti-His (Invitrogen), anti-GFP (Sigma-Aldrich), anti-actin (Sigma-Aldrich), or anti-HA (Covance) antibody.

RAS1 and *RAS2*

The *RAS1* and *RAS2* gene replacement constructs were generated by the ligation PCR approach (Zhao et al., 2004). The upstream and downstream fragments of *RAS1* were amplified with primer pairs RS1F1-RS1R2 and RS1F2-RS1R2 (Table 5), respectively. After ligation with the *hph* cassette, the *RAS1* gene replacement construct was amplified with primers RS1F1 and RS1R2 and directly transformed into protoplasts of 70-15. For *RAS2*, the upstream and downstream flanking sequences were amplified with primer pairs RS2F1-RS2R1 and RS2F2-RS2R2 (Table 5). After ligation with the *hph* cassette, the *RAS2* gene replacement construct was amplified with primers RA2F1 and RS2R2 and directly transformed into protoplasts of 70-15. The resulting PCR products also were cloned between the *Pst*I and *Not*I sites of pBluescript II KS+ (Stratagene) as the *RAS2* gene replacement construct pCX79.

For constructing the *RAS2*^{G23V} allele, a 2.6-kb fragment containing the *RAS2* gene was amplified with primers RASUF and RASUR with *pfu* (Stratagene) and cloned between the *Apa*I and *Not*I sites on pCB1004. The resulting vector was used as the template for mutagenesis with the QuickChange II site-directed mutagenesis kit (Stratagene). Primers RASGF and RASGR (Table 5) were used to introduce the GGT to GTC mutation in the *RAS2*^{G23V} mutant construct pCX66. The *RAS2*^{S28N} mutant construct pCX91 was generated with a similar approach with primers RAS1SF and RAS1SR (Table 5). The G23V mutation on pCX66 and S28N mutation on pCX91 were confirmed by sequence analysis. To remove the CAAX box (residues CVLM), *RAS2* was amplified with primers RAS1CF and RAS1CR from pCX66 and cloned into pCB1004 as pCX90. The RP27-*RAS2*^{G23V} construct pCX99 was generated by cloning the *RAS2*^{S28N} allele amplified with primers RAS1XF and RAS1XR into pKB04 (Bruno et al., 2004).

Accession Numbers

Sequence data from this article can be found in the GenBank/EMBL data libraries under accession numbers EAA52507 (*MST50*), EAA53749 (*RAS1*), EAA53026 (*RAS2*), and AF250928 (*CDC42* homolog).

Supplemental Data

The following materials are available in the online version of this article.

Supplemental Figure 1. Yeast Two-Hybrid Assays of the Interaction of Mst50 with Mgb1 and the Cdc42 Homolog.

Supplemental Figure 2. Enhanced Sensitivity of the *mst50* Mutant to Cell Wall Lytic Enzymes.

ACKNOWLEDGMENTS

We thank Larry Dunkle and Charles Woloshuk at Purdue University for critical reading of this manuscript, Martin Dickman for providing the DN CtRas construct, Sarah Tucker for assistance with constructing *MST50*-GFP fusions, and James Sweigard for discussions on *RAS1* and *RAS2*. This work was supported by a grant from the USDA National Research Initiative and by a grant from the National Science Foundation.

Received October 8, 2005; revised June 18, 2006; accepted September 22, 2006; published October 20, 2006.

REFERENCES

Adachi, K., and Hamer, J.E. (1998). Divergent cAMP signaling pathways regulate growth and pathogenesis in the rice blast fungus *Magnaporthe grisea.* Plant Cell **10,** 1361–1373.

Barbacid, M. (1987). Ras genes. Annu. Rev. Biochem. **56,** 779–827.

Barr, M.M., Tu, H., VanAelst, L., and Wigler, M. (1996). Identification of Ste4 as a potential regulator of Byr2 in the sexual response pathway of *Schizosaccharomyces pombe.* Mol. Cell. Biol. **16,** 5597–5603.

Bartel, P.L., Chien, C.T., Sternglanz, R., and Fields, S. (1993). Using the Two-Hybrid System to Detect Protein-Protein Interactions. (Oxford, UK: Oxford University Press).

Bhattacharjya, S., Xu, P., Gingras, R., Shaykhutdinov, R., Wu, C.L., Whiteway, M., and Ni, F. (2004). Solution structure of the dimeric SAM domain of MAPKKK Ste11 and its interactions with the adaptor protein Ste50 from the budding yeast: Implications for Ste11 activation and signal transmission through the Ste50-Ste11 complex. J. Mol. Biol. **344,** 1071–1087.

Bourett, T.M., Sweigard, J.A., Czymmek, K.J., Carroll, A., and Howard, R.J. (2002). Reef coral fluorescent proteins for visualizing fungal pathogens. Fungal Genet. Biol. **37,** 211–220.

Bruno, K.S., Tenjo, F., Li, L., Hamer, J.E., and Xu, J.R. (2004). Cellular localization and role of kinase activity of *PMK1* in *Magnaporthe grisea.* Eukaryot. Cell **3,** 1525–1532.

Chen, C.B., and Dickman, M.B. (2005). Proline suppresses apoptosis in the fungal pathogen *Colletotrichum trifolii.* Proc. Natl. Acad. Sci. USA **102,** 3459–3464.

Choi, W.B., and Dean, R.A. (1997). The adenylate cyclase gene *MAC1* of *Magnaporthe grisea* controls appressorium formation and other aspects of growth and development. Plant Cell **9,** 1973–1983.

Dean, R.A. (1997). Signal pathways and appressorium morphogenesis. Annu. Rev. Phytopathol. **35,** 211–234.

Dean, R.A., et al. (2005). The genome sequence of the rice blast fungus *Magnaporthe grisea.* Nature **434,** 980–986.

de Jong, J.C., McCormack, B.J., Smirnoff, N., and Talbot, N.J. (1997). Glycerol generates turgor in rice blast. Nature **389,** 244–245.

Dixon, K.P., Xu, J.R., Smirnoff, N., and Talbot, N.J. (1999). Independent signaling pathways regulate cellular turgor during hyperosmotic stress and appressorium-mediated plant infection by *Magnaporthe grisea.* Plant Cell **11,** 2045–2058.

D'Souza, C.A., and Heitman, J. (2001). Conserved cAMP signaling cascades regulate fungal development and virulence. FEMS Microbiol. Rev. **25,** 349–364.

Dufresne, M., and Osbourn, A.E. (2001). Definition of tissue-specific and general requirements for plant infection in a phytopathogenic fungus. Mol. Plant Microbe Interact. **14,** 300–307.

Ha, Y.S., Memmott, S.D., and Dickman, M.B. (2003). Functional analysis of Ras in *Colletotrichum trifolii.* FEMS Microbiol. Lett. **226,** 315–321.

Howard, R.J., Ferrari, M.A., Roach, D.H., and Money, N.P. (1991). Penetration of hard substrates by a fungus employing enormous turgor pressures. Proc. Natl. Acad. Sci. USA **88,** 11281–11284.

Jansen, G., Buhring, F., Hollenberg, C.P., and Rad, M.R. (2001). Mutations in the SAM domain of STE50 differentially influence the MAPH-mediated pathways for mating, filamentous growth and osmotolerance in *Saccharomyces cerevisiae.* Mol. Genet. Genomics **265,** 102–117.

Jenczmionka, N.J., Maier, F.J., Losch, A.P., and Schafer, W. (2003). Mating, conidiation and pathogenicity of *Fusarium graminearum*, the main causal agent of the head-blight disease of wheat, are regulated by the MAP kinase *GPMK1.* Curr. Genet. **43,** 87–95.

Johnson, P.E., and Donaldson, L.W. (2006). RNA recognition by the Vts1p SAM domain. Nat. Struct. Mol. Biol. **13,** 177–178.

Kido, M., Shima, F., Satoh, T., Asato, T., Kariya, K., and Kataoka, T. (2002). Critical function of the Ras-associating domain as a primary Ras-binding site for regulation of *Saccharomyces cerevisiae* adenylyl cyclase. J. Biol. Chem. **277,** 3117–3123.

Kim, C.A., and Bowie, J.U. (2003). SAM domains: Uniform structure, diversity of function. Trends Biochem. Sci. **28,** 625–628.

Kronstad, J., De Maria, A., Funnell, D., Laidlaw, R.D., Lee, N., de Sa, M.M., and Ramesh, M. (1998). Signaling via cAMP in fungi: Interconnections with mitogen-activated protein kinase pathways. Arch. Microbiol. **170,** 395–404.

Kwan, J.J., Warner, N., Maini, J., Tung, K.W.C., Zakaria, H., Pawson, T., and Donaldson, L.W. (2006). *Saccharomyces cerevisiae* Ste50 binds the MAPKKK Ste11 through a head-to-tail SAM domain interaction. J. Mol. Biol. **356,** 142–154.

Lee, N., D'Souza, C.A., and Kronstad, J.W. (2003). Of smuts, blasts, mildews, and blights: cAMP signaling in phytopathogenic fungi. Annu. Rev. Phytopathol. **41,** 399–427.

Lee, N., and Kronstad, J.W. (2002). *ras2* controls morphogenesis, pheromone response, and pathogenicity in the fungal pathogen *Ustilago maydis.* Eukaryot. Cell **1,** 954–966.

Lee, Y.H., and Dean, R.A. (1993). cAMP regulates infection structure formation in the plant pathogenic fungus *Magnaporthe grisea.* Plant Cell **5,** 693–700.

Li, L., Xue, C.Y., Bruno, K., Nishimura, M., and Xu, J.R. (2004). Two PAK kinase genes, *CHM1* and *MST20*, have distinct functions in *Magnaporthe grisea.* Mol. Plant Microbe Interact. **17,** 547–556.

Mayorga, M.E., and Gold, S.E. (2001). The *ubc2* gene of *Ustilago maydis* encodes a putative novel adaptor protein required for filamentous growth, pheromone response and virulence. Mol. Microbiol. **41,** 1365–1379.

Mey, G., Oeser, B., Lebrun, M.H., and Tudzynski, P. (2002). The biotrophic, non-appressorium-forming grass pathogen *Claviceps purpurea* needs a *FUS3/PMK1* homologous mitogen-activated protein kinase for colonization of rye ovarian tissue. Mol. Plant Microbe Interact. **15,** 303–312.

Mitchell, T.K., and Dean, R.A. (1995). The cAMP-dependent protein kinase catalytic subunit is required for appressorium formation and pathogenesis by the rice blast pathogen *Magnaporthe grisea.* Plant Cell **7,** 1869–1878.

Muller, P., Katzenberger, J.D., Loubradou, G., and Kahmann, R. (2003). Guanyl nucleotide exchange factor Sql2 and Ras2 regulate filamentous growth in *Ustilago maydis.* Eukaryot. Cell **2,** 609–617.

Nishimura, M., Park, G., and Xu, J.R. (2003). The G-beta subunit *MGB1* is involved in regulating multiple steps of infection-related morphogenesis in *Magnaporthe grisea.* Mol. Microbiol. **50,** 231–243.

Okazaki, N., Okazaki, K., Tanaka, K., and Okayama, H. (1991). The Ste4+ gene, essential for sexual differentiation of *Schizosaccharomyces pombe*, encodes a protein with a leucine zipper motif. Nucleic Acids Res. **19,** 7043–7047.

Pan, X.W., and Heitman, J. (2002). Protein kinase A operates a molecular switch that governs yeast pseudohyphal differentiation. Mol. Cell. Biol. **22,** 3981–3993.

Papadaki, P., Pizon, V., Onken, B., and Chang, E.C. (2002). Two Ras pathways in fission yeast are differentially regulated by two Ras guanine nucleotide exchange factors. Mol. Cell. Biol. **22,** 4598–4606.

Park, G., Bruno, K.S., Staiger, C.J., Talbot, N.J., and Xu, J.R. (2004). Independent genetic mechanisms mediate turgor generation and penetration peg formation during plant infection in the rice blast fungus. Mol. Microbiol. **53,** 1695–1707.

Park, S.H., Zarrinpar, A., and Lim, W.A. (2003). Rewiring MAP kinase pathways using alternative scaffold assembly mechanisms. Science **299,** 1061–1064.

Ponting, C.P., and Benjamin, D.R. (1996). A novel family of Ras-binding domains. Trends Biochem. Sci. **21,** 422–425.

Ptashne, M., and Gann, A. (2003). Imposing specificity on kinases. Science **299,** 1025–1027.

Rad, M.R., Jansen, G., Buhring, F., and Hollenberg, C.P. (1998). Ste50p is involved in regulating filamentous growth in the yeast *Saccharomyces cerevisiae* and associates with Ste11p. Mol. Genet. Genomics **259,** 29–38.

Ramezani-Rad, M. (2003). The role of adaptor protein Ste50-dependent regulation of the MAPKKK Ste11 in multiple signaling pathways of yeast. Curr. Genet. **43,** 161–170.

Raymond, C.K., Sims, E.H., and Olson, M.V. (2002). Linker-mediated recombinational subcloning of large DNA fragments using yeast. Genome Res. **12,** 190–197.

Rudoni, S., Colombo, S., Coccetti, P., and Martegani, E. (2001). Role of guanine nucleotides in the regulation of the Ras/cAMP pathway in *Saccharomyces cerevisiae.* Biochim. Biophys. Acta **1538,** 181–189.

Sesma, A., and Osbourn, A.E. (2004). The rice leaf blast pathogen undergoes developmental processes typical of root-infecting fungi. Nature **431,** 582–586.

Solomon, P.S., Waters, O.D.C., Simmonds, J., Cooper, R.M., and Oliver, R.P. (2005). The Mak2 MAP kinase signal transduction pathway is required for pathogenicity in *Stagonospora nodorum.* Curr. Genet. **48,** 60–68.

Talbot, N.J. (2003). On the trail of a cereal killer: Exploring the biology of *Magnaporthe grisea.* Annu. Rev. Microbiol. **57,** 177–202.

Talbot, N.J., Ebbole, D.J., and Hamer, J.E. (1993). Identification and characterization of *MPG1*, a gene involved in pathogenicity from the rice blast fungus *Magnaporthe grisea.* Plant Cell **5,** 1575–1590.

Talbot, N.J., Kershaw, M.J., Wakley, G.E., deVries, O.M.H., Wessels, J.G.H., and Hamer, J.E. (1996). *MPG1* encodes a fungal hydrophobin involved in surface interactions during infection-related development of *Magnaporthe grisea.* Plant Cell **8,** 985–999.

Truckses, D.M., Bloomekatz, J.E., and Thorner, J. (2006). The RA domain of Ste50 adaptor protein is required for delivery of Ste11 to the plasma membrane in the filamentous growth signaling pathway of the yeast *Saccharomyces cerevisiae.* Mol. Cell. Biol. **26,** 912–928.

Tu, H., Barr, M., Dong, D.L., and Wigler, M. (1997). Multiple regulatory domains on the Byr2 protein kinase. Mol. Cell. Biol. **17,** 5876–5887.

Tucker, S.L., and Talbot, N.J. (2001). Surface attachment and pre-penetration stage development by plant pathogenic fungi. Annu. Rev. Phytopathol. **39,** 385–419.

Tucker, S.L., Thornton, C.R., Tasker, K., Jacob, C., Giles, G., Egan, M., and Talbot, N.J. (2004). A fungal metallothionein is required for pathogenicity of *Magnaporthe grisea.* Plant Cell **16,** 1575–1588.

Valent, B., and Chumley, F.G. (1991). Molecular genetic analysis of the rice blast fungus *Magnaporthe grisea.* Annu. Rev. Phytopathol. **29,** 443–467.

Veneault-Fourrey, C., Barooah, M., Egan, M., Wakley, G., and Talbot, N.J. (2006). Autophagic fungal cell death is necessary for infection by the rice blast fungus. Science **312,** 580–583.

Veneault-Fourrey, C., and Talbot, N.J. (2005). Moving toward a systems biology approach to the study of fungal pathogenesis in the rice blast fungus *Magnaporthe grisea.* Adv. Appl. Microbiol. **57,** 177–215.

Wang, Y., Pierce, M., Schneper, L., Guldal, C.G., Zhang, X.Y., Tavazoie, S., and Broach, J.R. (2004). Ras and Gpa2 mediate one branch of a redundant glucose signaling pathway in yeast. PLoS Biology **2,** 610–622.

Waugh, M.S., Nichols, C.B., DeCesare, C.M., Cox, G.M., Heitman, J., and Alspaugh, J.A. (2002). Ras1 and Ras2 contribute shared and unique roles in physiology and virulence of *Cryptococcus neoformans.* Microbiol. **148,** 191–201.

Xu, G., Jansen, G., Thomas, D.Y., Hollenberg, C.P., and Rad, M.R. (1996). Ste50p sustains mating pheromone-induced signal transduction in the yeast *Saccharomyces cerevisiae.* Mol. Microbiol. **20,** 773–783.

Xu, J.R. (2000). MAP kinases in fungal pathogens. Fungal Genet. Biol. **31,** 137–152.

Xu, J.R., and Hamer, J.E. (1996). MAP kinase and cAMP signaling regulate infection structure formation and pathogenic growth in the rice blast fungus *Magnaporthe grisea.* Genes Dev. **10,** 2696–2706.

Xu, J.R., Peng, Y.L., Dickman, M.B., and Sharon, A. (2006). The dawn of fungal pathogen genomics. Annu. Rev. Phytopathol. **44,** 337–366.

Xue, C.Y., Park, G., Choi, W.B., Zheng, L., Dean, R.A., and Xu, J.R. (2002). Two novel fungal virulence genes specifically expressed in appressoria of the rice blast fungus. Plant Cell **14,** 2107–2119.

Zhao, X.H., Kim, Y., Park, G., and Xu, J.R. (2005). A mitogen-activated protein kinase cascade regulating infection-related morphogenesis in *Magnaporthe grisea.* Plant Cell **17,** 1317–1329.

Zhao, X.H., Xue, C., Kim, Y., and Xu, J.R. (2004). A ligation-PCR approach for generating gene replacement constructs in *Magnaporthe grisea.* Fungal Genet. Newsl. **51,** 17–18.